



OPEN Transcriptome changes induced by Arbuscular mycorrhizal symbiosis in leaves of durum wheat (*Triticum durum* Desf.) promote higher salt tolerance

Guglielmo Puccio^{1,4}✉, Rosolino Ingraffia^{1,2,3}✉, Francesco Mercati⁴✉, Gaetano Amato¹, Dario Giambalvo¹, Federico Martinelli⁵, Francesco Sunseri⁶ & Alfonso S. Frenda¹

The salinity of soil is a relevant environmental problem around the world, with climate change raising its relevance, particularly in arid and semiarid areas. Arbuscular Mycorrhizal Fungi (AMF) positively affect plant growth and health by mitigating biotic and abiotic stresses, including salt stress. The mechanisms through which these benefits manifest are, however, still unclear. This work aimed to identify key genes involved in the response to salt stress induced by AMF using RNA-Seq analysis on durum wheat (*Triticum turgidum* L. subsp. *durum* Desf. Husn.). Five hundred sixty-three differentially expressed genes (DEGs), many of which involved in pathways related to plant stress responses, were identified. The expression of genes involved in trehalose metabolism, RNA processing, vesicle trafficking, cell wall organization, and signal transduction was significantly enhanced by the AMF symbiosis. A downregulation of genes involved in both enzymatic and non-enzymatic oxidative stress responses as well as amino acids, lipids, and carbohydrates metabolisms was also detected, suggesting a lower oxidative stress condition in the AMF inoculated plants. Interestingly, many transcription factor families, including WRKY, NAC, and MYB, already known for their key role in plant abiotic stress response, were found differentially expressed between treatments. This study provides valuable insights on AMF-induced gene expression modulation and the beneficial effects of plant-AMF interaction in durum wheat under salt stress.

Soil salinity is one of the most severe environmental stresses in agricultural systems due to its adverse effects on crop growth and productivity¹. Approximately 20% of cultivated and almost 30% of irrigated lands are affected by soil salinization². High salt deposition in soil affects plant development by inducing physiological, biochemical, and molecular modifications, resulting in cellular osmotic stress, and ionic and redox imbalances. Plants evolved several mechanisms to avoid damage due to salt stress, mainly by ion-homeostasis, solute accumulation, water and nutrient uptake regulation, and ROS detoxification through antioxidant enzymes and molecules^{3–5}. The interactions between plants and microorganisms (Plant-Growth-Promoting microorganisms and Arbuscular Mycorrhizal Fungi—AMF) are also reported to play a key role in the crop yield maintenance under stress environments^{6,7}.

More than 80% of land plants, including several crop species, are symbiotically associated with AMF⁸. This symbiosis positively impacts plant health and the ability to mitigate both biotic and abiotic stresses through

¹Department of Agricultural, Food and Forestry Sciences, University of Palermo, Palermo, Italy. ²Plant Ecology, Institute of Biology, Freie Universität Berlin, Berlin, Germany. ³Berlin-Brandenburg Institute of Advanced Biodiversity Research, Berlin, Germany. ⁴Institute of Biosciences and BioResources (IBBR), National Research Council of Italy, Palermo, Italy. ⁵Department of Biology, University of Florence, Sesto Fiorentino, Italy. ⁶Department of Agraria, University Mediterranea of Reggio Calabria, Reggio Calabria, Italy. ✉email: gupuccio@gmail.com; rosolino.ingraffia@unipa.it; francesco.mercati@ibbr.cnr.it

several mechanisms, such as root architecture change, higher accumulation of osmolytes, enhancement of the antioxidant defense system, maintenance of ion homeostasis, and higher photosynthetic efficiency^{9–14}. The plant ability to explore a higher soil volume due to the fungal hyphae results in a higher water and nutrient (P, N, Mg, and Ca) uptake by mycorrhizal plants^{15–17}. These positive effects could be attributable to an increased expression of many genes involved in plant nutrition in AMF colonized plants. Indeed, genes related to proline, trehalose, soluble sugars, and other osmolytes are often upregulated in mycorrhizal plants to contrast cell dehydration caused by the lower turgor^{18,19}. In addition, AMF symbiosis is also responsible for increased enzymatic and non-enzymatic oxidative stress responses by the upregulation of peroxidases (POX), catalases (CAT), and superoxide dismutase (SOD) and by increasing the synthesis of antioxidant compounds²⁰. A Na⁺ and Cl⁻ high concentration in the soil can also lead to harmful ionic imbalances. AMF were reported to enhance ion homeostasis by regulating organic acids and polyamines concentration as well as enhancing Na⁺/K⁺ and Na⁺/H⁺ transporters (HKT, NHX and SOS) expression, to support Na⁺ efflux from cytosol to apoplast or into the vacuole²¹. Furthermore, nitrogen (N) plays a crucial role in mitigating the salt stress^{22,23}. Soil salinity can stimulate the expression of NO₃⁻ transporters and increase NR activity, according to many gene expression analyses^{24–26}. Indeed, the accumulation of N-containing metabolites is an important strategy to mitigate both osmotic and oxidative stress²⁷. Interestingly, these processes are often enhanced by AMF root colonization resulting in the higher expression of plant NRT transporters and proton ATPases²⁸. All these mechanisms help mycorrhizal plants to cope with soil salinity resulting in improved plant growth compared to the uninoculated plants.

Although many efforts have been made in recent years to improve knowledge of the complex mechanisms underlying salt stress response in model plants^{29,30}, few studies have focused on transcriptional regulation in non-model plants, including durum wheat. The agronomic, metabolic and proteomic responses to salt stress in durum and bread wheat have been described^{31,32}, while the transcriptional changes induced by salinity were reported mainly in the bread wheat (*Triticum aestivum*) roots^{33–35}. Targeted comparative analysis of transcripts abundance by qPCR on durum wheat under salt stress and its mitigation effect by AMF symbiosis have been reported^{26,36}. Interestingly, a positive effect of AMF symbiosis on plant biomass, N uptake, and plasma membranes stability in durum wheat under salt stress were detected²⁶, highlighting also a significant drought-related genes downregulation in the AMF-inoculated plants.

A wide comparative transcriptomic analysis between AMF inoculated and uninoculated durum wheat plants grown under salt stress will help to better understand the mechanisms involved in salinity stress tolerance mediated by AMF symbiosis.

Thus, after assessing the effects of mycorrhization on productive and qualitative traits of durum wheat grown under salt stress, the putative key genes involved in the improved response of mycorrhizal plants to salt stress were identified using RNA-seq analysis.

Results

Effects of arbuscular mycorrhizal fungi on durum wheat plants grown under salinity stress. The mycorrhizal colonization of uninoculated plants was very negligible (on average 0.5% of the root length colonized with values always < 1%), whereas it was, on average, 31.2% (p value < 0.0001) in inoculated plants. AM + plants showed significantly higher aboveground and root biomass and total N uptake compared to the uninoculated (AM-) plants (+ 9.2%, + 32.1%, and 21.5% respectively; Fig. 1). Moreover, AM + plants had a higher membrane stability index (MSI) value compared to the AM- plants (+ 12.5% on average).

Differential gene expression analysis. A RNA-Seq analysis on both Arbuscular Mycorrhizal fungi inoculated (AM+) and uninoculated durum wheat plants (AM-) grown under salt stress was performed to identify key pathways involved in the AMF-induced salt tolerance.

Three hundred eleven (311) million single-end (SE) reads were obtained, with an average of 51 million reads per sample. Two hundred and seventy-eight (278) million reads were mapped to the durum wheat genome with an average of 77% mapping reads per sample. Five hundred and sixty-three (563) Differentially Expressed Genes (DEGs) between AM + and AM- samples were found, of which 277 with a log₂FC < -1 and 270 with a log₂FC > 1 (down- and upregulated by the AMF colonization, respectively) (Fig. 2A,B, Table S1). DEGs were distributed in all the seven chromosomes of both sub-genomes A and B. Their chromosome abundance was correlated with chromosome length (Pearson correlation, r = 0.83), and significant differences were not found between the sub-genomes (267 and 280 DEGs located on sub-genome A and B, respectively). The highest and lowest number of DEGs were found on chromosomes 3B (54) and 6A (21), respectively (Fig. 2C).

By using the durum wheat genome ncRNA annotation, lncRNAs were also investigated. Five lncRNA Differentially Expressed (DE) between treatments (Fig. 3B), two upregulated (STRG.778651, STRG.1311431) and three downregulated (STRG.234623, STRG.424631, STRG.1760891) by the AMF colonization were found. Interestingly, all the lncRNA DE were located on the sub-genome B in chromosomes 1, 2, 3, 5, and 7 and annotated using the RNACentral sequence search tool (<https://rnacentral.org/sequence-search/>) (Table S2).

Transcriptomic profile modification induced by AMF symbiosis. DEGs analysis between treatments revealed many genes involved in salt stress-related pathways such as ion transport and binding, response to oxidative and abiotic stress, calcium signaling, and osmolytes accumulation. AMF symbiosis significantly increased the expression levels of many genes previously reported as related to AMF-induced salt stress tolerance¹² (Table 1). Concurrently a significant decrease in the expression of genes involved in the response to oxidative stress, GABA metabolism as well as ions and oligopeptides transport was observed. In particular, in the AM + samples, two catalase (CAT), two Glutathione S-transferase (GST), and twelve Cytochrome P450 (CYP) genes, all belonging to the enzymatic antioxidative systems, resulted downregulated. Furthermore, seven

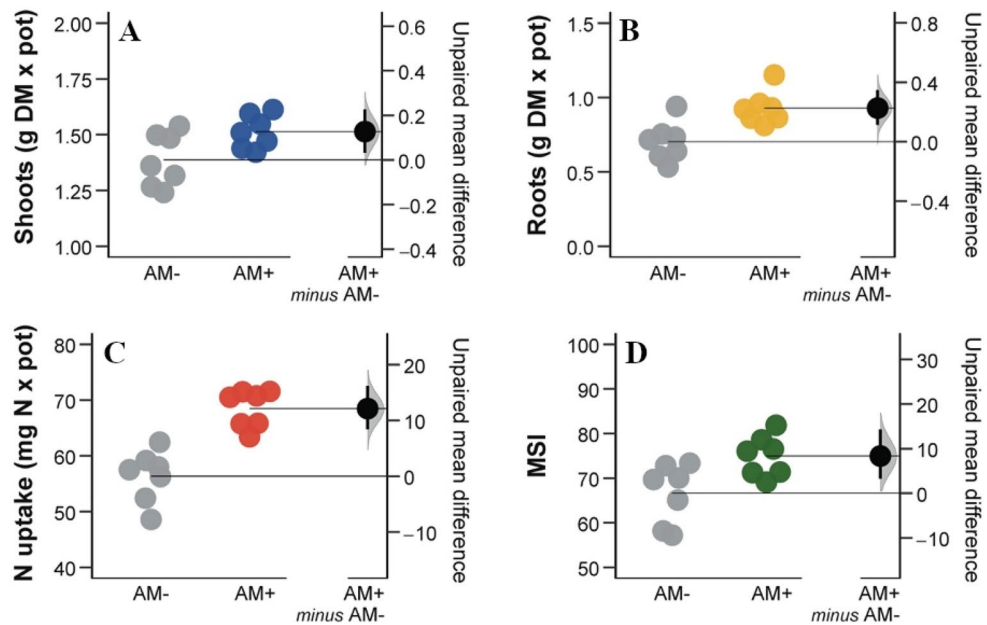


Figure 1. Shoot (A) and root (B) biomass, total N uptake (C) and membrane stability index (MSI; D). Raw data of Control (AM-, grey dots) and arbuscular mycorrhizal treatment (AM+, coloured dots) are shown in the plot. The filled curve indicates the resampled distribution of unpaired mean difference for AM+ minus AM-, given the observed data. Horizontally aligned with the mean of the test group (AM+), unpaired mean difference is indicated by the black circle. The 95% confidence intervals of each difference is illustrated by the black vertical lines.

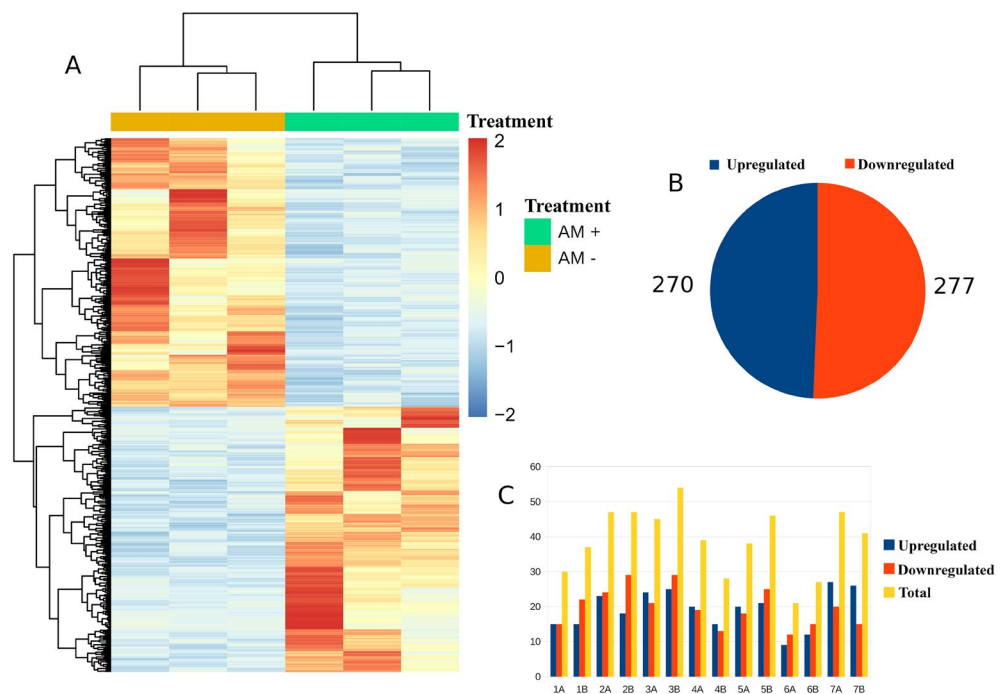


Figure 2. Overview of differential expression analysis performed with DESeq2. Heatmap of the normalized expression levels of the 563 Differentially Expressed Genes (DEGs) between the AM+ and AM- conditions generated using the pheatmap R package (<https://cran.r-project.org/web/packages/pheatmap/index.html>; version 1.0.12) (A). Number of Differentially expressed genes in the two conditions (B). Distribution of DEGs in the 7 chromosomes of the *Triticum durum* genome (C).

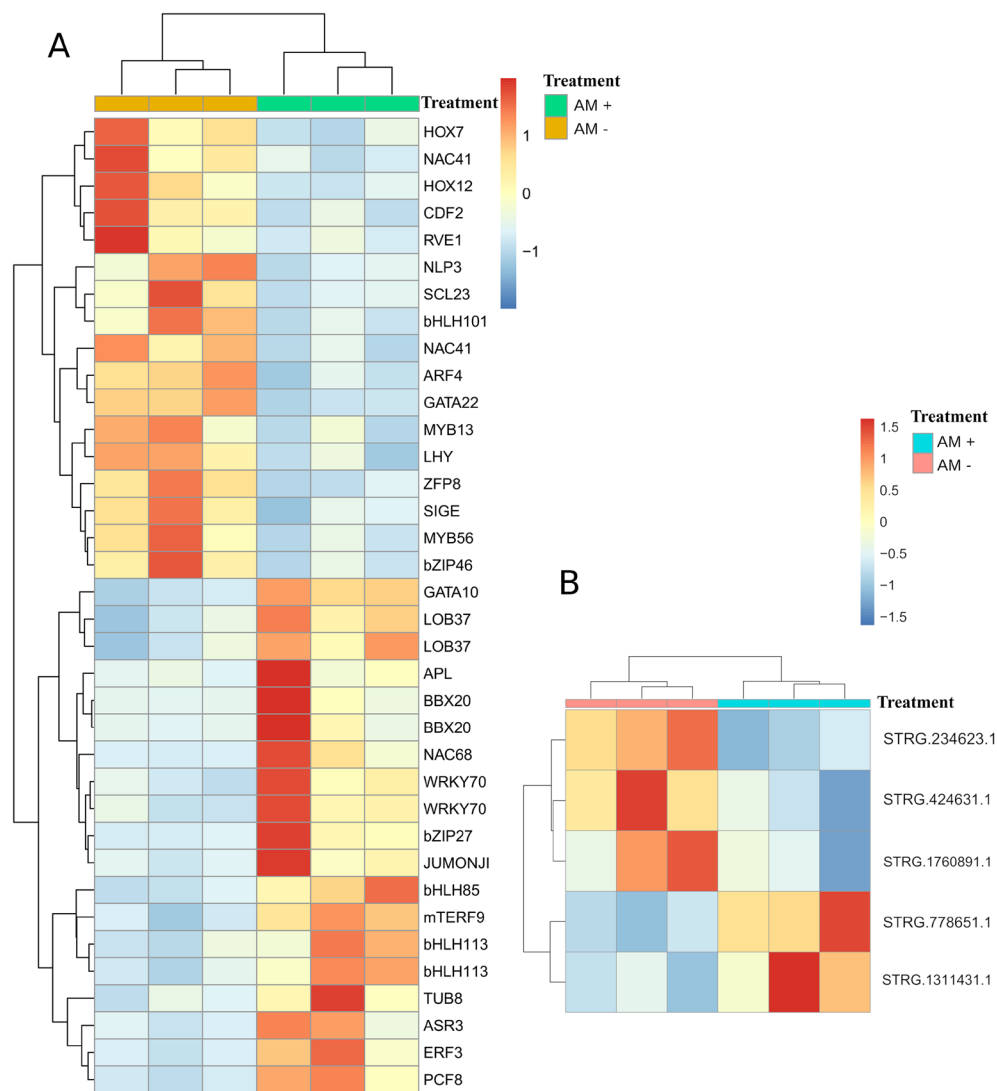


Figure 3. Expression patterns and hierarchical clustering of the 36 Transcription Factors identified comparing the AM+ (green) and AM- (yellow) conditions (A). Heatmap showing the lncRNA differentially expressed under salt stress in the AM+ (blue) and AM- (pink) conditions (B). Both heatmaps were generated using the pheatmap R package (<https://cran.r-project.org/web/packages/pheatmap/index.html>; version 1.0.12).

peroxidases (POX), also involved in the response to oxidative stress, were found DE (four upregulated and three downregulated).

Interestingly, genes involved in osmoregulation and osmolytes accumulation such as sugars, amino acids, and trehalose were also modulated by AMF. In AM+ plants, the expression of three sugar efflux transporters (SWEET) and eight invertases (beta-fructofuranosidase), involved in the conversion of sucrose to fructose and glucose, two ADP-glucose pyrophosphorylases and two polyamine oxidases (PAO) was significantly reduced. Furthermore, AMF colonization significantly enhanced the expression of a trehalose-6-P synthase (TPS) and two trehalose-6-P phosphatases (TPP), both responsible of trehalose biosynthesis, by contrast the trehalose degrading enzyme, trehalase (TRE), did not appear differentially expressed between treatments. Modulation of ion transporters genes is a key process for regulating the accumulation and compartmentalization of both ions and solutes. Four amino acid transporters (ANT and LHT) (two up- and two down-regulated) and twelve lipid-transfer proteins (eight up- and four down-regulated) were found differentially expressed. AMF symbiosis also enhanced the expression of a Tonoplast Intrinsic Protein (TIP) aquaporin, as well as ten transporter genes, including two borate transporters (BOR). By contrast, twenty-four transporter genes were significantly downregulated by the AMF colonization. Many of these are involved in amino acids, oligopeptides, and sodium transport such as three anion transporters, two auxin transporters, (PIN, PILS), two sodium HKT, two ABC transporters, and two oligopeptide transporters (OPT).

Among the nitrate transporters, five NPF and a NRT2 gene involved in both low- and high-affinity nitrate transport were differentially expressed between treatments. In detail, *NRT2.2* and three *NPF5* were down-regulated in AM+ samples while a *NPF7* and a *NPF8* genes resulted upregulated.

	Triticum durum gene ID	Log ₂ FC	P-value	Padj	Transcript description
Oxidoreduction	TRITD6Av1G007920	-2.2	3.9E-09	4.4E-06	Catalase
	TRITD6Bv1G012280	-2.1	9.3E-08	6.2E-05	Catalase
	TRITD3Av1G174080	-1.2	4.6E-05	7.4E-03	Glutathione S-transferase
	TRITD3Av1G263790	-1.7	6.2E-06	1.7E-03	Glutathione S-transferase
Osmoregulation	TRITD3Av1G171110	-1.7	1.1E-04	1.4E-02	Bidirectional sugar transporter SWEET
	TRITD3Bv1G149640	-1.6	7.7E-04	4.9E-02	Bidirectional sugar transporter SWEET
	TRITD7Bv1G019190	-2.1	4.0E-04	3.2E-02	Bidirectional sugar transporter SWEET
	TRITD1Bv1G219480	-2.1	1.3E-06	5.4E-04	Glucose-1-phosphate adenylyltransferase
	TRITD1Av1G222050	-2.2	2.0E-05	3.9E-03	Glucose-1-phosphate adenylyltransferase
	TRITD7Av1G204550	-2.8	3.9E-05	6.7E-03	Polyamine oxidase 1
	TRITD7Bv1G158080	-3.7	8.3E-09	8.2E-06	Polyamine oxidase
Transporters	TRITD4Bv1G194950	2.2	1.3E-05	2.8E-03	Aquaporin-like protein (TIP)
	TRITD3Av1G042320	-1.3	2.9E-04	2.6E-02	ABC transporter
	TRITD5Av1G221130	-1.5	4.2E-04	3.3E-02	ABC transporter
	TRITD6Bv1G179870	-1.3	1.5E-05	3.3E-03	Auxin efflux carrier component (PIN)
	TRITD5Bv1G152290	-2.5	1.3E-05	2.8E-03	Auxin efflux carrier family protein (PILS)
	TRITD5Av1G044900	1.4	1.0E-04	1.3E-02	Boron transporter
	TRITD5Bv1G042780	1.9	2.5E-04	2.3E-02	Boron transporter
	TRITD2Av1G215440	1.4	6.5E-04	4.4E-02	Mitochondrial Ca ²⁺ uptake protein
	TRITD6Av1G057110	1	6.7E-04	4.5E-02	Calcium-transporting ATPase
	TRITD6Bv1G067420	1	4.7E-04	3.5E-02	Calcium-transporting ATPase
	TRITD2Av1G032000	-2.2	8.7E-07	3.9E-04	Cation calcium exchanger
	TRITD2Bv1G041270	-1.7	5.2E-05	7.9E-03	Cation calcium exchanger
	TRITD7Av1G226260	-1.2	4.5E-05	7.4E-03	HKT23 transporter
	TRITD7Bv1G172350	-1	6.8E-04	4.5E-02	HKT23 transporter
	TRITD1Bv1G205440	-1.7	2.1E-06	7.7E-04	Oligopeptide transporter
	TRITD1Bv1G205480	-1.6	9.3E-05	1.2E-02	Oligopeptide transporter
	NPF-NRT2	TRITD2Av1G001860	-1.7	6.2E-05	9.0E-03
TRITD4Bv1G191460		-1.4	1.8E-05	3.7E-03	NPF transporter 5
TRITD5Av1G243130		-1.8	1.7E-09	2.0E-06	NPF transporter 5
TRITD6Bv1G164770		2.8	3.1E-04	2.7E-02	NPF transporter 7
TRITD2Bv1G262700		1.1	1.0E-04	1.3E-02	NPF transporter 5
TRITD7Bv1G180680		-1.9	1.6E-04	1.7E-02	NRT2.2
Glutamate metabolic pathway	TRITD2Av1G208370	1.6	6.6E-04	4.5E-02	Glutamate decarboxylase
	TRITD4Bv1G016030	0.9	6.2E-04	4.3E-02	Glutamate decarboxylase
	TRITD7Bv1G022320	-7.4	1.2E-07	7.4E-05	Glutamate receptor
Trehalose metabolic pathway	TRITD5Bv1G123710	2.8	7.0E-06	1.9E-03	Trehalose-6-phosphate synthase
	TRITD6Av1G158120	1.2	2.4E-04	2.3E-02	Trehalose 6-phosphate phosphatase
	TRITD6Bv1G144550	1.1	1.4E-04	1.5E-02	Trehalose 6-phosphate phosphatase
MAP Kinases	TRITD2Av1G270510	2	7.8E-06	2.0E-03	Protein kinase (MAP3K)
	TRITD6Bv1G202800	2.9	4.2E-06	1.3E-03	Protein kinase (MAPKK)
	TRITD2Av1G187690	1.2	5.5E-04	3.9E-02	Protein kinase (MAP3K)
Calcium signaling	TRITD5Bv1G079480	1.2	2.1E-04	2.1E-02	Calmodulin binding protein
	TRITD2Av1G044340	-1.6	3.4E-06	1.1E-03	CIPK21
	TRITD2Bv1G037460	-1.4	2.8E-07	1.4E-04	CIPK2
	TRITD5Bv1G024270	-2.8	1.5E-05	3.2E-03	CIPK4
Other	TRITD3Av1G219080	2.2	2.2E-04	2.2E-02	Early response to dehydration 15-like
	TRITD3Bv1G211690	2.2	1.9E-04	2.0E-02	Early response to dehydration 15-like
	TRITD7Bv1G038640	1.3	4.6E-04	3.5E-02	Late embryogenesis abundant protein
	TRITD4Bv1G187750	1.5	8.4E-05	1.1E-02	Late embryogenesis abundant protein
	TRITD4Bv1G187770	2.4	4.5E-10	7.7E-07	Late embryogenesis abundant protein
	TRITD7Av1G099670	1.4	6.2E-05	9.0E-03	RAB GTPase
	TRITD3Bv1G206370	1.3	5.1E-04	3.7E-02	RAB GTPase

Table 1. Key genes involved in the response to salt stress found differentially expressed between AM + and AM- samples. Log₂ Fold Change (Log₂FC), P-value, and Deseq2 adjusted P-value (Padj) are shown.

In AM + plants, several genes involved in calcium signaling, such as calcium dependent transporters like Ca^{2+} /cation exchanger (CCX) and Mitochondrial Ca^{2+} Uptake proteins (MICU), as well as three calcium-dependent protein kinases, *CIPK2*, *CIPK4*, and *CIPK21*, were found downregulated, while two P2B Ca^{2+} ATPase (*ACA*) and a calmodulin binding protein were upregulated. Furthermore, three genes involved in GABA metabolism, a GABA transaminase (*GABA-T*) and two glutamate decarboxylases (*GAD*), involved in GABA synthesis from glutamic acid, were also downregulated. Finally, in AM + plants, RAB GTPases, Late Embryogenesis Abundant (*LEA*) proteins, proline-rich proteins (*PRP*), and two MAP kinases (*MAP2K*, *MAP3K*) were significantly upregulated.

Transcription Factors modulated by AMF symbiosis. The characterization of the expression profiles of Transcription Factors (TFs) is a crucial step in RNA-Seq analyses; here, thirty-six TFs were differentially expressed between treatments, of which 17 and 19 up- and down-regulated, respectively in AM + plants (Fig. 3A, Table S3). Many upregulated TFs were often involved in the response to abiotic and drought stress such as *WRKY*, Dehydration Responsive Element Binding (*DREB*), Early Response to Dehydration 15 like (*ERD15*), and *bHLH*. Among the downregulated TFs, two MYB genes (*MYB13* and *MYB56*), two NAC, and an Auxin Response Factor (*ARF4*) were identified.

Profile validation of DEGs via qPCR. RNA-seq results were validated by qPCR using five randomly selected genes, two up- (*LEA* and *NRT1*), and three down-regulated (*HKT*, *MYB*, and *NRT2.2*). Their expression profiles were normalized to the housekeeping gene (Table S5). The expression trend of selected genes in qPCR (Fig. S2) appeared in agreement with the RNA-Seq expression levels. Pearson's correlation coefficients were evaluated between RNA-seq and qPCR results showed high correlation and significance ($R = 0.89$; $p < 0.0001$).

Gene Ontology (GO) and MapMan analysis. GO terms for Biological Process (BP), Molecular Function (MF) and Cellular Component (CC), were assigned to all the 563 DEGs and the enrichment analysis for both upregulated and downregulated genes was performed by using PANTHER.

In the BP category, enriched GO terms were not shared between the two sets of DEGs (up- and down-regulated by AMF inoculation). Many terms highly correlated to abiotic stress response such as “response to stress”, “response to stimulus”, “response to hydrogen peroxide”, “oxidation–reduction process”, “cell wall macromolecule catabolic process” and “lipid metabolic process” were found enriched in the downregulated genes set (Fig. 4). By contrast, the upregulated genes were mainly enriched in the GO terms “macromolecule modification”, “protein phosphorylation”, “protein autophosphorylation”, “phosphorus metabolic process”, “cellular macromolecule metabolic process” and “cell wall biogenesis”.

In the MF category, “molecular function” and “catalytic activity” terms were shared between up- and down-regulated genes by AMF (Fig. S3). In addition, the downregulated genes were enriched in “hydrolase activity” and “oxidoreductase activity” terms, while three “purine binding” related terms, together with “ion binding”, “anion binding” and “carbohydrate derivative binding” terms were found enriched in the upregulated genes.

In the CC category, the “protein–containing complex” term was enriched in both up- and down-regulated sets of DEGs being also the only term enriched in the downregulated set (Fig. S4). Finally, other six terms were enriched in the upregulated genes, among which “cell wall”, “cell periphery” and “external encapsulating structure” appeared the most representative.

MapMan analysis highlighted the main metabolic pathways and functional groups involved in the response to salt stress comparing AM + and AM– treatments (Fig. S5). Three hundred eighty-nine out of 563 DEGs were correctly assigned to already known metabolic pathways. In detail, downregulated genes by AMF symbiosis were mainly involved in the amino acids biosynthesis and degradation, lipid metabolism, redox homeostasis process, terpenoids biosynthesis, phytohormone transport and biosynthesis as well as carbohydrate metabolism. By contrast, genes induced by AMF inoculation were mainly involved in RNA processing, vesicle trafficking, protein biosynthesis and cytoskeleton organization. Genes involved in solute transport, cell wall organization, RNA biosynthesis and external stimuli response were found in both up- and down-regulated genes sets.

Co-expression network analysis. The differentially expressed TFs panel to perform a co-expression network analysis highlighting specific interactions between key TFs and putative target genes was used. Only the TFs with a sub-network of at least two genes were considered for further analysis (six out of 36 were discarded). The network contains 230 co-expressed genes including 28 TFs that define a main sub-network of 122 genes and 11 TFs (4 and 7 up- and downregulated, respectively) and 9 smaller sub-networks (Fig. 5, Table S4). The main sub-network showed negative correlation between several TFs and their co-expressed genes, suggesting a TF repressive regulation. *zFP8* and *GATA10* TFs showed the highest number of connections inside the main network (hub genes). More interestingly, many DEGs previously mentioned for their important role in the salt stress response were found co-expressed together with some TFs utilized as baits. A *HKT* and *PIN* auxin transporter and a *TPP* gene resulted co-expressed to both *GATA* TFs. Both *BBX20* like TFs were connected to the up-regulated ERDs and a *TPP* gene, while *zFP8* with many OPTs, 5 Thaumatin-like proteins, and the *CIPK2* gene. Finally, a F-box (*TRITD1Av1G225260*) and a RING/U-box (*TRITD4Av1G177780*) genes, both involved in the ubiquitination process, were co-expressed with *bZIP27*.

Discussion

Soil salinity is a relevant abiotic stress that can drastically limit crop growth and yield. High salt concentration in the soil is known to induce osmotic and oxidative stress and nutrient deficiency. Indeed, salinity can alter photosynthesis rates, cellular osmotic and ionic homeostasis through redox imbalances and accumulation of toxic elements (i.e., Na^+ and Cl^-), and can inhibit protein synthesis and deplete cellular energy.

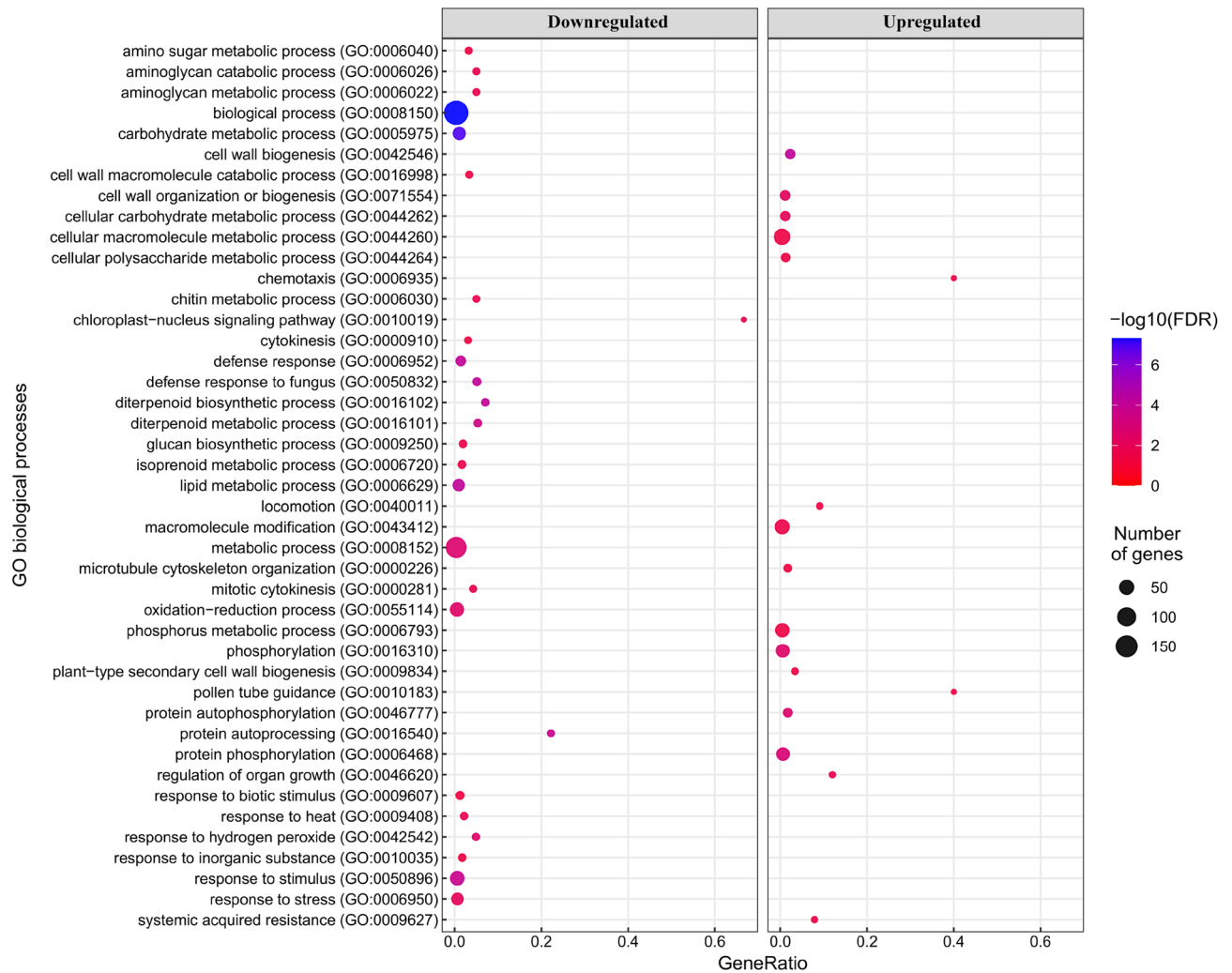


Figure 4. Biological Processes GO terms enrichment analysis for upregulated and downregulated genes. The dot plot shows enriched GO terms ($\text{FDR} < 0.05$) identified with PANTHER using the Fisher's exact test. The size of the dots represents the number of genes in each GO biological process while the GeneRatio (x-axis) is the ratio between the number of DEGs found and the number of genes in that category.

Our findings showed that AMF symbiosis can mitigate the adverse effects of salt stress on durum wheat growth. In particular, we found that AM symbiosis favored N acquisition, and above- and below-ground plant growth under salt stress condition, in agreement with previous studies, as reviewed by Evelin et al.¹². Moreover, we detected a clear positive effect of AM symbiosis on the alleviation of the damaging effects of salinity on the stability of plasma membranes. Abiotic stresses primarily target the cell membrane, and it is generally believed that maintaining their integrity and stability under stress conditions is a major component of salt stress tolerance in plants. We, therefore, concluded that mycorrhizal plants are more resistant to salinity stress than their non-mycorrhizal counterparts.

Non-colonized wheat plants exposed to salt stress showed lower MSI values than colonized plants, partially due to the salt affecting the electrical potential of the plasma membrane. As a result of AMF symbiosis, we observed a beneficial effect on MSI, which reduced the need to activate plants salt stress response mechanisms. Thus, AM + plants appeared subjected to a lower level of salt stress compared to AM- plants.

Several studies underlined the ability of AMF symbiosis to enhance plant salt tolerance by genes transcription modulation both in roots and shoot under different experimental conditions^{4,12,21}. The protective effect of AMF under stress such as salinity, drought, and heat were already reported in durum and bread wheat^{34,37,38}. Here, we described for the first time the differential transcriptomic profile of durum wheat leaves under salt stress with and without AMF inoculation. RNA-seq data were useful to describe the molecular mechanisms induced by AMF colonization to mitigate the salt stress in durum wheat. The identified DEGs between treatments revealed novel insights into the role of AMF symbiosis in the plant response to salt stress.

Soil salinity induces ROS formation and their accumulation both in roots and shoot tissues resulting in oxidative damage of cellular components. Plants react to ROS formation either by an enzymatic and non-enzymatic antioxidative system³⁹. The enzymatic system determines a higher superoxide dismutase (SOD), catalase (CAT), glutathione reductase, and S-transferases (GR, GST), as well as peroxidase (POX) accumulation, while the non-enzymatic system involves the synthesis of antioxidant molecules such as ascorbate, carotenoids, and glutathione

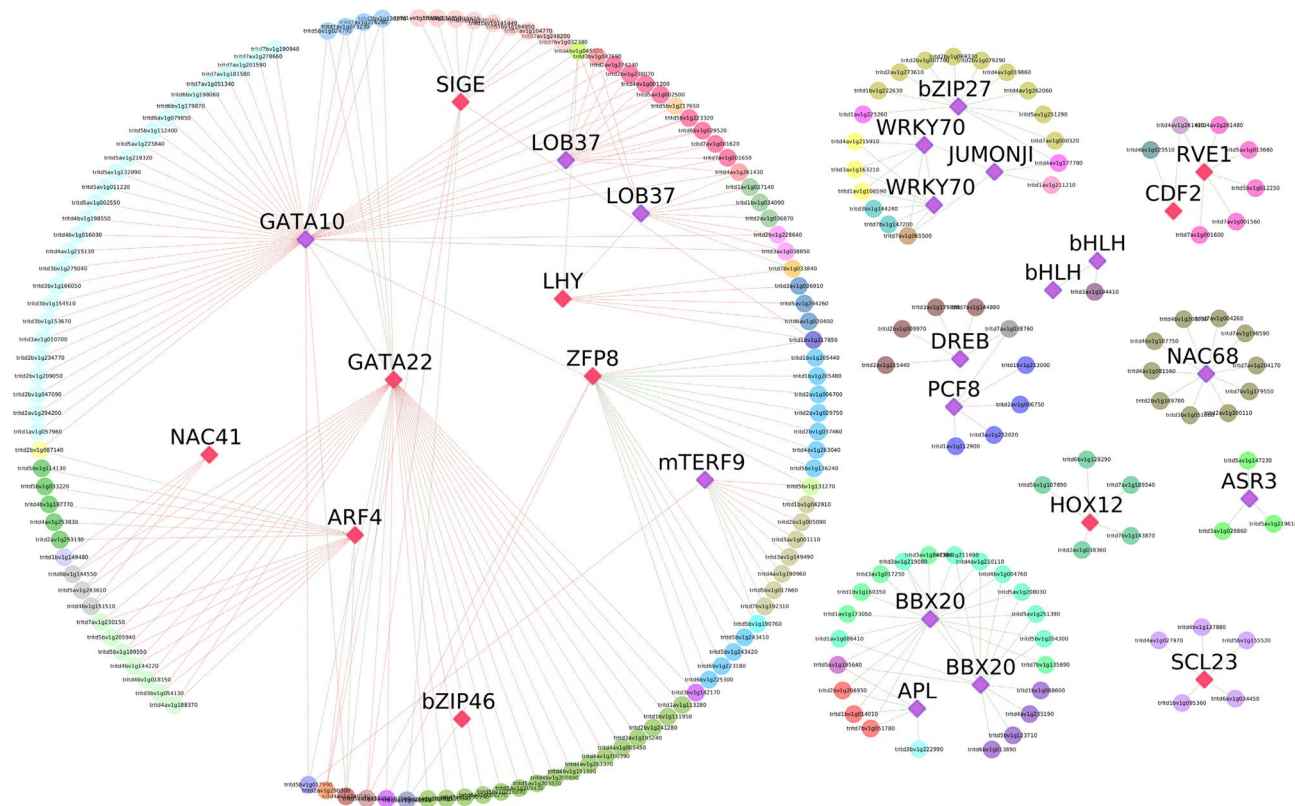


Figure 5. Co-expression network analyses of 30 Transcription Factors (TF) differentially expressed under salt stress as bait genes. The network was obtained with CoExpNetViz tool and visualized by Cytoscape. Bait TFs are represented as squared nodes. Colors represents downregulated TFs (red) and upregulated TFs (violet) while green and red lines denote positive correlation and negative correlation, respectively. Nine sub-networks are present, with the bigger one including 122 genes and 11 TFs.

to counteract ROS accumulation toxicity²⁰. In the present study, a higher number of enzymes involved in redox reactions such as CATs, GSTs, and CYPs significantly downregulated in the leaves of AM+ plants were found. Thus, the AMF symbiosis ability to suppress Na⁺'s antagonistic effect, reducing ROS accumulations, which could result in lower cellular and thylakoidal membranes damage, was suggested. CATs are involved in the enzymatic response to ROS⁴⁰, GSTs reduce oxidative stress by affecting glutathione pools^{41,42}, while CYP genes are known to provide tolerance to salinity and other abiotic stresses by influencing ROS scavenging and ABA levels⁴³. Both GABA and glutamate metabolism and catabolism were also reported to play a key role in the response to salt stress by controlling ROS accumulation and regulating redox balance^{44,45}. Interestingly, in AM+ plants, we detected a significant downregulation of two glutamate or Glutamic Acid Decarboxylase (GAD) enzymes involved in the synthesis of GABA from L-glutamate as well as a GABA-T involved in the conversion of GABA to succinic semialdehyde (SSA), already reported to be induced by salt stress in Arabidopsis and maize^{46,47}.

Otherwise, N-compounds have been suggested to contribute to osmo-protective processes and to mitigate oxidative stress by scavenging ROS²³. Here, three NPF transporters and a NRT2 transporter resulted downregulated by the AMF symbiosis. In agreement, a significant reduction in the expression of genes involved in the N uptake was induced by ectomycorrhizal fungi inoculation in poplar²⁸; by contrast, tomato plants under both drought and salt stress showed a NRT2 gene⁴⁸ upregulation^{28,48}. In our condition, AM+ plants exhibited an improved ability to uptake and translocate N, resulting in a reduced expression of high-affinity transporters in leaves probably due to a higher nitrate level in the xylem.

Two HKT genes involved in the Na⁺ transport from shoot to roots, thus able to remove Na⁺ from the xylem appeared significantly downregulated in the AM+ samples, in contrast with previous findings in which the AMF symbiosis determined their upregulation²¹. HKTs down-regulation may suggest a higher ionic balance in the AM+ plants in agreement with Estrada et al.⁴⁹ that measured a higher K⁺/Na⁺ ratio in AM+ samples as well as a higher state of oxidative stress in AM- samples. This last condition may be caused by an inefficient water and ionic homeostasis, highlighted by enriched GO terms identified in the downregulated genes such as "oxidation-reduction process" and "response to stress". The reduction of plant defense responses to salt stress in the oxidation-reduction reactions observed in the shoot of AM+ compared to AM- plants is probably due to their healthier condition.

To mitigate the adverse effects of the low soil water potential caused by salinity, plants accumulate osmolytes such as proline, betaine, polyamines, sugars, organic acids, amino acids, and trehalose, aiding the water flow from the soil into the roots and then to shoots¹². Higher osmotic potential in AM+ compared to AM- plants

has been already reported⁵⁰. In our study, a high number of Proline-Rich Proteins (PRPs) upregulated by the AMF symbiosis were detected. These seem to be involved in cell wall stress-induced fortification as confirmed by six cell wall-related GO terms enriched in the upregulated genes, including “cell wall biogenesis” and “cell wall organization”. Indeed, proline is an important osmo-protectant, accumulated under salt stress as free proline or in PRPs, mainly in cell walls^{51,52}. Trehalose is a non-reduced storage disaccharide that may serve as energy and carbon source, seeming also involved in both ROS scavenging and K⁺/Na⁺ ratio maintenance⁵³. A higher levels of trehalose in legume grown under salt stress were reported⁵⁴. In agreement, a trehalose-6-P synthase (TPS) and two trehalose-6-P phosphatases (TPP), involved in the trehalose synthesis, resulted strongly upregulated in AM + durum wheat plants.

Moreover, several genes involved in polyamines and carbohydrates metabolisms resulted downregulated by AMF inoculum, in agreement to the GO term “carbohydrate metabolic process”, significantly enriched in the downregulated genes set. Polyamines are important regulators of cellular ROS homeostasis⁵⁵, while the accumulation of soluble carbohydrates was detected in the leaves of salt stressed sorghum plants⁵⁶.

Changes in cytosolic free Ca²⁺ concentration are known to be involved in message transduction and response to several external stimuli, biotic and abiotic stresses^{57,58}. During drought and salt stress, a high number of calcium-related genes involved in the Ca²⁺ signaling pathway are induced. In our comparison, a calmodulin-binding protein and two P2B Ca²⁺ATPase, both responsible for the active Ca²⁺ transport and homeostasis, were upregulated by the AMF symbiosis. More interestingly, these genes were already reported as involved in salt stress responses in moss, soybean, and rice plants^{59–62}. Finally, three MAPKs, involved in different signaling cascades including Ca²⁺, resulted upregulated in the AM + plants.

In our condition, the AMF colonization downregulated three CIPKs and two Ca²⁺/cation exchangers (CCX). Interestingly, CIPKs are involved in Ca²⁺ signal transduction in abiotic stress responses in many crops^{57,63,64}, by contrast, the role of CCXs is still scarcely characterized. They localize to the vacuolar or plasma membrane and could be involved in Na⁺/K⁺ exchange and stress response having been found highly upregulated during both salt and drought stress in many plants, despite limited knowledge on their regulation and specific functions is available until now^{65–67}.

The aquaporins form a large protein family with a pivotal role in plant water use efficiency (WUE) and water transport. A complex transcriptional pattern of aquaporins under salt stress has been described in several crops^{68–70}. Both Tonoplastic and Protoplastic Intrinsic Proteins (TIPs and PIPs), involved in the intracellular and transcellular water transport, respectively, under salt stress were found modulated by the AM fungi both in roots and leaves⁷¹. Here, we identified a TIP gene upregulated by the AMF inoculation.

Many transcription factors belonging to DREB, NAC, MYB, bHLH, bZIP, ERF, BBX, and WRKY families play a significant role in biotic and abiotic stress plant responses^{72–75}. We identified seventeen TFs upregulated by the AMF symbiosis among which two *WRKY70* homologs, a *DREB*, a *NAC68* homolog, and two *bHLH*. The overexpression of WRKY, NAC, and DREB members were able to enhance abiotic and biotic stress responses in rice, *Arabidopsis* and *Nicotiana benthamiana*^{76–79}. In wheat, the overexpression of both *NAC29* and *bZIP15* has been recently reported to enhance salt stress response by reducing H₂O₂ accumulation^{80,81}. Furthermore, two *BBX20* TFs were significantly upregulated by the AMF symbiosis in our experiment, in agreement with the higher expression of this family members previously reported in several plants under salt and heat stress^{82,83}.

In our condition, *MYB13* and *MYB56* were also identified among the downregulated TFs in AM + plants, and both members were reported to induce drought, salt, and cold stress tolerance in transgenic *Arabidopsis*^{84,85}, suggesting a lower oxidative stress level.

Interestingly, RAB-A, LEA, and ERD genes were identified among the upregulated DEGs induced by AMF inoculation. RAB-A GTPases are involved in membrane trafficking, and signal transduction and appeared involved in salt stress tolerance^{86,87}. Members belonging to the LEA gene family enhanced salt and dehydration stress tolerance when overexpressed in transgenic plants^{88–90}. LEA proteins have been also reported to act as a molecular shield during abiotic stresses avoiding protein aggregation and preventing enzyme degradation⁹¹.

Finally, long noncoding RNAs (lncRNAs) have been found frequently induced during abiotic stress plant responses^{92–94}. Here, we detected two lncRNAs upregulated and three down-regulated by the AMF symbiosis under salt stress. Interestingly, the ortholog of a drought-responsive lncRNA (URS0000781584) identified in maize by Zhang et al. resulted downregulated in our experiment⁹⁵.

In conclusion, we observed a lower number of stress-related genes modulated by soil salinity in AM + compared to AM– samples. This appears in agreement with the results previously obtained on bread and durum wheat^{26,34}, supporting the hypothesis of a salt stress mitigation induced by AMF symbiosis. The DEGs identified in our condition included plant defensive genes against redox state (i.e., cytochrome P450, glutathione S-transferase, catalases) and were involved in osmoregulation, osmolytes, and ions transport. These observations were confirmed by the GO-term enrichment analysis that showed categories related to stresses (i.e., “response to stress”, “response to hydrogen peroxide”, and “oxidation–reduction process”) significantly enriched in AM-plants. More interestingly, MapMan analysis identified a higher number of genes involved in pathways related to abiotic stress responses such as amino acids and carbohydrate biosynthesis and metabolism (involved in osmotic regulation), lipid metabolism (dehydration protection), redox homeostasis process (anti-radical responses), terpenoids biosynthesis (antioxidant protection) and phytohormone transport (stress response modulation). Finally, the co-expression network analysis was able to identify many TFs acting as hub-genes in the regulation of the higher salt tolerance mediated by AMF-inoculum in durum wheat.

Altogether, our molecular findings well correlate with a higher salt stress tolerance previously observed in AM + plants and may be considered a gene atlas that clearly sustains a healthier status of AMF colonized compared to non-colonized plants. Further studies will be necessary to narrow down the genes set here identified to isolate candidate major genes involved in AMF-mediated salt tolerance for further functional analyses. The

adoption of different AMF species, salt concentrations, and times of exposure to stress may help to improve our knowledge on the interaction between plants and AMF.

Methods

Plant material and experimental design. Durum wheat (*Triticum durum* Desf. cv. Anco Marzio) plants were grown outdoors in pots under salt stress with and without AMF inoculation (namely 'AM+' and 'AM-', respectively). A complete randomized design was adopted with seven replicates (for a total of 14 pots). Each pot (diameter 150 mm, height 130 mm) was filled with 2000 g of a quartz sand:soil mixture (1:1). Soil properties were as follows: 267 g kg⁻¹ clay, 247 g kg⁻¹ silt, and 486 g kg⁻¹ sand; pH 8.0; 6.3 g kg⁻¹ total carbon (C); 0.86 g kg⁻¹ total N; available P (Olsen) 40.1 mg kg⁻¹; 1.70 dS m⁻¹ saturated electrical conductivity (EC) (25 °C). Both soil and sand were sieved through a 2 mm mesh and autoclaved at 121 °C for 20 min to completely impair soil biological (both fungal and bacterial) activity. The native bacterial microflora was extracted by suspending 500 g of fresh soil in 1.5 l distilled water. After shaking and decanting, the suspension was filtered (11 µm mesh) to discard the native AMF community. Each pot received 30 ml of soil suspension filtrate to reintroduce the native microbial community before AMF inoculation, performed with 10 g per pot rate of a commercial AMF inoculum (AEGIS IRRIGA, Italtollina SpA, Rivoli Veronese, Italy), consisting of a *Rhizophagus irregularis* and *Funnelformis mosseae* spore mixture, at 700 spores g⁻¹ of inoculum rate for each. The commercial inoculum also contains 1 × 10⁷ rhizosphere bacteria. To isolate the AMF effects, we extracted the bacterial community belonging to the inoculum, using the same protocol applied for the native soil microbial community reported above, and introduced it to the AM- treatment. The microbial inoculations were performed at the same time as sowing. The native microbiome and the bacterial community present in the inoculum (only for AM- treatment) were added in liquid form as reported above, while AM fungal inoculum was distributed just below the sowing bed. Each pot received 60 mg of N in the form of ammonium sulfate ([NH₄]₂SO₄).

Sixteen seeds, previously surface-sterilized with H₂O₂ at 4% for 3 min, were sown in each pot. Ten days after emergence, plants were thinned to six seedlings per pot. The plantlets were grown for 15 days before the application of salt to avoid its negative effect on the AMF symbiosis establishment. Salt stress was determined by adding NaCl to the irrigation water (10 g l⁻¹). To prevent osmotic shock, salt was added gradually by distributing in total 1 l of NaCl solution in each pot within seven days from the beginning of the salinity treatment. This treatment led the EC of saturated soil extract to 13.00 dS m⁻¹. Afterward, plants were watered with tap water (0.58 dS m⁻¹) until harvest. Leaching was avoided by maintaining soil water always below field capacity. During the experiment, the irrigation was performed every 2 days and the amount of irrigation water consisted of the total replenishment of water lost through evapotranspiration for each pot.

All pots were harvested after 45 days from sowing. Plant aboveground biomass was immediately separated into stems, green leaves, and senescent and dry leaves, and the fresh weight of each fraction was recorded. Root biomass was extracted by carefully cutting the pots vertically and removing the substrate by washing. About 1 g of green leaves and 1 g of roots from each pot were immediately frozen in liquid N, stored at -80 °C, and subsequently pulverized without thawing. At the same time, a sample of green full expanded leaves (about 400 mg) was taken from each pot to determine the membrane stability index (MSI). The leaf material was divided into two sets of 200 mg each. The first set was heated at 40 °C for 30 min in a water bath (10 cm³); then the electrical conductivity bridge (C1) was measured. The second set was boiled at 100 °C for 10 min (in 10 cm³ of water) before measuring the electrical conductivity bridge (C2). MSI was calculated according to Sairam et al.⁹⁶

A representative root sample (about 1 g) was taken from each pot to determine the overall colonization of roots by AM fungi. To this end, root samples were cleared in KOH and stained with trypan blue following the method described by Phillips et al.⁹⁷. AM fungi root colonization was then measured with the grid intersect method⁹⁸.

Plant N content was determined separately on dry material of each botanical fraction obtained as previously described using the combustion method of Dumas (DuMaster D-480, Büchi Labortechnik AG, Flawil, Switzerland). For each pot, total N uptake was calculated as the sum of N accumulated in roots (root dry mass × root N concentration) and shoots (shoot dry mass × shoot N concentration).

All plant data were compared between the two groups (AM+ and AM-) using the dabestr R package⁹⁹ to generate unpaired mean differences via a bias-corrected and accelerated bootstrapped 95% Confidence Intervals (Cis). Graphical data representations were generated using the dabestr R package. All analyses were performed using R version 4.0.2¹⁰⁰.

RNA-Seq library preparation and sequencing. Total RNA from leaves using the Spectrum Plant Total RNA kit (Sigma) and treated with RNase-free DNase was isolated. RNA quantification was analyzed by the Nanodrop ND-1000 (Thermo Scientific, Waltham, MA, USA) and its quality (RNA integrity number—RIN > 8.0) was assessed using an Agilent Bioanalyzer RNA nanochip (Agilent, Wilmington, DE, USA). Three biological replicates for each treatment were used. Each replicate included a pool of healthy fully expanded leaves taken from all the plants in the pots. Sequence libraries were prepared as reported in Puccio et al.¹⁰¹ using a TruSeq RNA Sample Preparation Kit v2 (Illumina, San Diego, CA, USA). Both quality and insert size distribution by using an Agilent Bioanalyzer DNA 1000 chip were assessed. Sequence libraries were pooled in equimolar concentration and analyzed on an Illumina HiSeq 2000 generating 75 bp reads. The generated sequences were deposited in the NCBI (National Center for Biotechnology Information) SRA database with the accession: PRJNA746118.

Reads pre-processing and mapping. The quality assessment of reads obtained from both AM inoculated (AM+) and non-inoculated (AM-) samples were performed using the FastQC tool v0.11.8¹⁰². Sequence

trimming was not performed and the high sequencing quality with a median per base sequence quality of 36 (Phred Score) and the absence of adapter sequences was reported (Fig. S1). Reads were mapped to the newly released *Triticum turgidum* L. ssp. *durum* genome¹⁰³ using STAR¹⁰⁴ with default parameters and assigned to genomic features using featureCounts¹⁰⁵ with default parameters.

Differential expression analysis and annotation. Differentially expressed genes (DEGs) and long non-coding RNA (lncRNA) between treatments were obtained using the DESeq2 R package, using an adjusted p-value (padj) < 0.05 as threshold¹⁰⁶. DEGs were annotated using the *Triticum durum* genome annotation, the *Triticum aestivum* orthologues from the biomart plants database, the online PANTHER functional classification¹⁰⁷ and visualized using the pheatmap R package (version 1.0.12)¹⁰⁸. DEGs were also assigned to specific metabolic pathways using the online functional annotator Mercator¹⁰⁹ and visualized with MapMan¹¹⁰. Furthermore, differentially expressed (DE) lncRNA were annotated using the nhmmer function of the online database RNACentral¹¹¹.

GO enrichment and co-expression network analysis. GO enrichment analysis was performed with PANTHER overrepresentation test using the Fisher's exact test and a False Discovery Rate (FDR) threshold of 0.05. Enriched GO terms were then filtered with the REVIGO tool¹¹² to reduce GO terms redundancy and visualized using the R package ggplot2¹¹³.

A Co-expression network analysis was performed by the CoExpNetViz tool¹¹⁴ using the 1st and 99th percentiles of the Pearson correlation coefficients distribution, as thresholds. Differentially expressed (DE) transcription factors (TFs) were used as bait genes while the entire set of DEGs was used as pool. The Network obtained was visualized and analyzed using Cytoscape¹¹⁵ using the network analyzer tool.

RNA-Seq analysis validation using qPCR. To validate the results from the RNAseq analyses, a set of five genes were randomly selected among DEGs (Table S5) and tested by qPCR, using the actin gene as reference¹¹⁶. Primer 3.0 software (<http://primer3.ut.ee/>) (accessed on 16 October 2021) to design primer pair for each selected gene was utilized (Table S5). Total RNA from leaves of durum wheat plants belonging to an independent experiment performed following the same procedures described in “Plant material and experimental design” section was isolated. Reverse transcription was performed on 200 ng of total RNA extracted from AM- and AM+ samples, using iScript Reverse Transcription Supermix (Bio-Rad, Berkeley, CA, USA), according to manufacturer's instructions. qPCR was performed as described in Puccio et al.¹⁰¹, starting from 20 ng of cDNA¹⁰¹. Three biological and three technical replicates were analyzed for each sample (AM+ and AM-). Fragment amplification was verified by 1.5% w/v agarose gel electrophoresis and melting curve analysis. The relative expression ratio of each gene was calculated by the $2^{-\Delta\Delta CT}$ method¹¹⁷. Pearson correlation analysis between RNA-Seq and qPCR was also performed.

Legislation statement. All procedures were conducted in accordance to the institutional, national, and international guidelines and legislation.

Data availability

The datasets supporting the conclusions of this article are available in the Sequence Read Archive (SRA) repository (<http://www.ncbi.nlm.nih.gov/sra/>), accession number: PRJNA746118.

Received: 31 July 2022; Accepted: 21 December 2022

Published online: 03 January 2023

References

- Rengasamy, P. World salinization with emphasis on Australia. *J. Exp. Bot.* **57**, 1017–1023 (2006).
- Shahid, S. A., Zaman, M. & Heng, L. Soil salinity: Historical perspectives and a world overview of the problem. In *Guideline for Salinity Assessment, Mitigation and Adaptation Using Nuclear and Related Techniques* 43–53 (Springer, 2018).
- Munns, R. & Tester, M. Mechanisms of salinity tolerance. *Annu. Rev. Plant Biol.* **59**, 651–681 (2008).
- Ruiz-Lozano, J. M., Porcel, R., Azcón, C. & Aroca, R. Regulation by arbuscular mycorrhizae of the integrated physiological response to salinity in plants: New challenges in physiological and molecular studies. *J. Exp. Bot.* **63**, 4033–4044 (2012).
- Augé, R. M., Toler, H. D. & Saxton, A. M. Arbuscular mycorrhizal symbiosis and osmotic adjustment in response to NaCl stress: A meta-analysis. *Front. Plant Sci.* **5**, 562 (2014).
- Singh, R. P., Jha, P. & Jha, P. N. The plant-growth-promoting bacterium *Klebsiella* sp. SBP-8 confers induced systemic tolerance in wheat (*Triticum aestivum*) under salt stress. *J. Plant Physiol.* **184**, 57–67 (2015).
- Vimal, S. R., Singh, J. S., Arora, N. K. & Singh, S. Soil-plant-microbe interactions in stressed agriculture management: A review. *Pedosphere* **27**, 177–192 (2017).
- Smith, S. E. & Read, D. J. *Mycorrhizal Symbiosis* (Academic Press, 2010).
- Pozo, M. J., Jung, S. C., López-Ráez, J. A. & Azcón-Aguilar, C. Impact of arbuscular mycorrhizal symbiosis on plant response to biotic stress: The role of plant defence mechanisms. In *Arbuscular Mycorrhizas: Physiology and Function* 193–207 (Springer, 2010).
- Bitterlich, M., Roupheal, Y., Graefe, J. & Franken, P. Arbuscular mycorrhizas: A promising component of plant production systems provided favorable conditions for their growth. *Front. Plant Sci.* **9**, 1329 (2018).
- Chandrasekaran, M., Chanratana, M., Kim, K., Seshadri, S. & Sa, T. Impact of arbuscular mycorrhizal fungi on photosynthesis, water status, and gas exchange of plants under salt stress—A meta-analysis. *Front. Plant Sci.* **10**, 457 (2019).
- Evelin, H., Devi, T. S., Gupta, S. & Kapoor, R. Mitigation of salinity stress in plants by arbuscular mycorrhizal symbiosis: Current understanding and new challenges. *Front. Plant Sci.* **10**, 470 (2019).
- Begum, N. et al. Role of arbuscular mycorrhizal fungi in plant growth regulation: Implications in abiotic stress tolerance. *Front. Plant Sci.* **10**, 1068 (2019).

14. Alaux, P.-L., Naveau, F., Declerck, S. & Cranenbrouck, S. Common mycorrhizal network induced JA/ET genes expression in healthy potato plants connected to potato plants infected by *Phytophthora infestans*. *Front. Plant Sci.* **11**, 602 (2020).
15. Saia, S., Amato, G., Frenda, A. S., Giambalvo, D. & Ruisi, P. Influence of arbuscular mycorrhizae on biomass production and nitrogen fixation of berseem clover plants subjected to water stress. *PLoS One* **9**, 90738 (2014).
16. Ingrassia, R., Amato, G., Frenda, A. S. & Giambalvo, D. Impacts of arbuscular mycorrhizal fungi on nutrient uptake, N₂ fixation, N transfer, and growth in a wheat/faba bean intercropping system. *PLoS One* **14**, e0213672 (2019).
17. Ingrassia, R. *et al.* Nitrogen type and availability drive mycorrhizal effects on wheat performance, nitrogen uptake and recovery, and production sustainability. *Front. Plant Sci.* **11**, 760 (2020).
18. Evelin, H., Giri, B. & Kapoor, R. Ultrastructural evidence for AMF mediated salt stress mitigation in *Trigonella foenum-graecum*. *Mycorrhiza* **23**, 71–86 (2013).
19. Alqarawi, A. A., Abd Allah, E. F. & Hashem, A. Alleviation of salt-induced adverse impact via mycorrhizal fungi in *Ephedra aphylla* Forssk. *J. Plant Interact.* **9**, 802–810 (2014).
20. Gill, S. S. & Tuteja, N. Reactive oxygen species and antioxidant machinery in abiotic stress tolerance in crop plants. *Plant Physiol. Biochem.* **48**, 909–930 (2010).
21. Porcel, R., Aroca, R., Azcon, R. & Ruiz-Lozano, J. M. Regulation of cation transporter genes by the arbuscular mycorrhizal symbiosis in rice plants subjected to salinity suggests improved salt tolerance due to reduced Na⁺ root-to-shoot distribution. *Mycorrhiza* **26**, 673–684 (2016).
22. Ruiz-Lozano, J. M., Azcon, R. & Gomez, M. Alleviation of salt stress by arbuscular-mycorrhizal *Glomus* species in *Lactuca sativa* plants. *Physiol. Plant* **98**, 767–772 (1996).
23. Mansour, M. M. F. Nitrogen containing compounds and adaptation of plants to salinity stress. *Biol. Plant.* **43**, 491–500 (2000).
24. Popova, O. V., Dietz, K.-J. & Gollack, D. Salt-dependent expression of a nitrate transporter and two amino acid transporter genes in *Mesembryanthemum crystallinum*. *Plant Mol. Biol.* **52**, 569–578 (2003).
25. Nie, L. *et al.* Comparative proteomics of root plasma membrane proteins reveals the involvement of calcium signalling in NaCl-facilitated nitrate uptake in *Salicornia europaea*. *EXBOTJ* **66**, 4497–4510 (2015).
26. Fileccia, V. *et al.* Arbuscular mycorrhizal symbiosis mitigates the negative effects of salinity on durum wheat. *PLoS One* **12**, e0184158 (2017).
27. Shabala, S. Learning from halophytes: Physiological basis and strategies to improve abiotic stress tolerance in crops. *Ann. Bot.* **112**, 1209–1221 (2013).
28. Sa, G. *et al.* Amelioration of nitrate uptake under salt stress by ectomycorrhiza with and without a Hartig net. *New Phytol.* **222**, 1951–1964 (2019).
29. Porcel, R. *et al.* Arbuscular mycorrhizal symbiosis ameliorates the optimum quantum yield of photosystem II and reduces non-photochemical quenching in rice plants subjected to salt stress. *J. Plant Physiol.* **185**, 75–83 (2015).
30. Zhou, Y. *et al.* Transcriptome analysis of salt stress responsiveness in the seedlings of Dongxiang wild rice (*Oryza rufipogon* Griff.). *PLoS ONE* **11**, e0146242 (2016).
31. Almansouri, M., Kinet, J.-M. & Lutts, S. Effect of salt and osmotic stresses on germination in durum wheat (*Triticum durum* Desf.). *Plant Soil* **231**, 243–254 (2001).
32. Capriotti, A. L. *et al.* Proteomic study of a tolerant genotype of durum wheat under salt-stress conditions. *Anal. Bioanal. Chem.* **406**, 1423–1435 (2014).
33. El-Amri, S. M., Al-Whaibi, M. H., Abdel-Fattah, G. M. & Siddiqui, M. H. Role of mycorrhizal fungi in tolerance of wheat genotypes to salt stress. *Afr. J. Microbiol. Res.* **7**, 1286–1295 (2013).
34. Talaat, N. B. & Shawky, B. T. Protective effects of arbuscular mycorrhizal fungi on wheat (*Triticum aestivum* L.) plants exposed to salinity. *Environ. Exp. Bot.* **98**, 20–31 (2014).
35. Zhu, X., Song, F., Liu, S., Liu, F. & Li, X. Arbuscular mycorrhiza enhances nutrient accumulation in wheat exposed to elevated CO₂ and soil salinity. *J. Plant Nutr. Soil Sci.* **181**, 836–846 (2018).
36. Annunziata, M. G. *et al.* Durum wheat roots adapt to salinity remodeling the cellular content of nitrogen metabolites and sucrose. *Front. Plant Sci.* **7**, 2035 (2017).
37. Beltrano, J. & Ronco, M. G. Improved tolerance of wheat plants (*Triticum aestivum* L.) to drought stress and rewatering by the arbuscular mycorrhizal fungus *Glomus claroideum*: Effect on growth and cell membrane stability. *Braz. J. Plant Physiol.* **20**, 29–37 (2008).
38. Cabral, C., Ravnkov, S., Tringovska, I. & Wollenweber, B. Arbuscular mycorrhizal fungi modify nutrient allocation and composition in wheat (*Triticum aestivum* L.) subjected to heat-stress. *Plant Soil* **408**, 385–399 (2016).
39. Ahmad, P., Jaleel, C. A., Salem, M. A., Nabi, G. & Sharma, S. Roles of enzymatic and nonenzymatic antioxidants in plants during abiotic stress. *Crit. Rev. Biotechnol.* **30**, 161–175 (2010).
40. Gondim, F. A., Gomes-Filho, E., Costa, J. H., Alencar, N. L. M. & Prisco, J. T. Catalase plays a key role in salt stress acclimation induced by hydrogen peroxide pretreatment in maize. *Plant Physiol. Biochem.* **56**, 62–71 (2012).
41. Qi, Y. C. *et al.* Overexpression of glutathione S-transferase gene increases salt tolerance of Arabidopsis. *Russ. J. Plant Physiol.* **57**, 233–240 (2010).
42. Chen, J.-H. *et al.* Drought and salt stress tolerance of an Arabidopsis glutathione S-transferase U17 knockout mutant are attributed to the combined effect of glutathione and abscisic acid. *Plant Physiol.* **158**, 340–351 (2012).
43. Pandian, B. A., Sathishraj, R., Djanaguiraman, M., Prasad, P. V. & Jugulam, M. Role of cytochrome P450 enzymes in plant stress response. *Antioxidants* **9**, 454 (2020).
44. Singh, M., Singh, A., Prasad, S. M. & Singh, R. K. Regulation of plants metabolism in response to salt stress: An omics approach. *Acta Physiol. Plant.* **39**, 48 (2017).
45. Wu, X. *et al.* Gamma-aminobutyric acid (GABA) alleviates salt damage in tomato by modulating Na⁺ uptake, the GAD gene, amino acid synthesis and reactive oxygen species metabolism. *BMC Plant Biol.* **20**, 1–21 (2020).
46. Renault, H. *et al.* The Arabidopsis pop2-1 mutant reveals the involvement of GABA transaminase in salt stress tolerance. *BMC Plant Biol.* **10**, 1–16 (2010).
47. Wang, Y. *et al.* γ-Aminobutyric acid imparts partial protection from salt stress injury to maize seedlings by improving photosynthesis and upregulating osmoprotectants and antioxidants. *Sci. Rep.* **7**, 1–13 (2017).
48. Akbudak, M. A., Filiz, E. & Çetin, D. Genome-wide identification and characterization of high-affinity nitrate transporter 2 (NRT2) gene family in tomato (*Solanum lycopersicum*) and their transcriptional responses to drought and salinity stresses. *J. Plant Physiol.* **272**, 153684 (2022).
49. Estrada, B., Aroca, R., Maathuis, F. J. M., Barea, J. M. & Ruiz-Lozano, J. M. Arbuscular mycorrhizal fungi native from a Mediterranean saline area enhance maize tolerance to salinity through improved ion homeostasis. *Plant Cell Environ.* **36**, 1771–1782 (2013).
50. Navarro, J. M., Pérez-Tornero, O. & Morte, A. Alleviation of salt stress in citrus seedlings inoculated with arbuscular mycorrhizal fungi depends on the rootstock salt tolerance. *J. Plant Physiol.* **171**, 76–85 (2014).
51. Ueda, A., Yamamoto-Yamane, Y. & Takabe, T. Salt stress enhances proline utilization in the apical region of barley roots. *Biochem. Biophys. Res. Commun.* **355**, 61–66 (2007).
52. Stein, H. *et al.* Elevation of free proline and proline-rich protein levels by simultaneous manipulations of proline biosynthesis and degradation in plants. *Plant Sci.* **181**, 140–150 (2011).

53. Redillas, M. C. F. R. *et al.* Accumulation of trehalose increases soluble sugar contents in rice plants conferring tolerance to drought and salt stress. *Plant Biotechnol. Rep.* **6**, 89–96 (2012).
54. Garg, N. & Pandey, R. High effectiveness of exotic arbuscular mycorrhizal fungi is reflected in improved rhizobial symbiosis and trehalose turnover in *Cajanus cajan* genotypes grown under salinity stress. *Fungal Ecol.* **21**, 57–67 (2016).
55. Saha, J. *et al.* Polyamines as redox homeostasis regulators during salt stress in plants. *Front. Environ. Sci.* **3**, 21 (2015).
56. de Lacerda, C. F., Cambraia, J., Oliva, M. A. & Ruiz, H. A. Changes in growth and in solute concentrations in sorghum leaves and roots during salt stress recovery. *Environ. Exp. Bot.* **54**, 69–76 (2005).
57. Xiang, Y., Huang, Y. & Xiong, L. Characterization of stress-responsive CIPK genes in rice for stress tolerance improvement. *Plant Physiol.* **144**, 1416–1428 (2007).
58. Batistič, O. & Kudla, J. Analysis of calcium signaling pathways in plants. *Biochim. Biophys. Acta BBA. Gen. Subj.* **1820**, 1283–1293 (2012).
59. Chung, W. S. *et al.* Identification of a calmodulin-regulated soybean Ca²⁺-ATPase (SCA1) that is located in the plasma membrane. *Plant Cell* **12**, 1393–1407 (2000).
60. Qudeimat, E. *et al.* A PIIB-type Ca²⁺-ATPase is essential for stress adaptation in *Physcomitrella patens*. *Proc. Natl. Acad. Sci.* **105**, 19555–19560 (2008).
61. Huda, K. M. K. *et al.* Os ACA 6, a P-type IIB Ca²⁺ ATPase promotes salinity and drought stress tolerance in tobacco by ROS scavenging and enhancing the expression of stress-responsive genes. *Plant J.* **76**, 997–1015 (2013).
62. Sun, M. *et al.* Functional characterization of a Glycine soja Ca²⁺ ATPase in salt-alkaline stress responses. *Plant Mol. Biol.* **90**, 419–434 (2016).
63. Sánchez-Barrena, M. J., Martínez-Ripoll, M., Zhu, J.-K. & Albert, A. The structure of the *Arabidopsis thaliana* SOS3: Molecular mechanism of sensing calcium for salt stress response. *J. Mol. Biol.* **345**, 1253–1264 (2005).
64. Hu, D. *et al.* Overexpression of MdsOS2L1, a CIPK protein kinase, increases the antioxidant metabolites to enhance salt tolerance in apple and tomato. *Physiol. Plant.* **156**, 201–214 (2016).
65. Amagaya, K., Shibuya, T., Nishiyama, M., Kato, K. & Kanayama, Y. Characterization and expression analysis of the Ca²⁺/cation antiporter gene family in tomatoes. *Plants* **9**, 25 (2020).
66. Singh, A. *et al.* Genome-wide expressional and functional analysis of calcium transport elements during abiotic stress and development in rice. *FEBS J.* **281**, 894–915 (2014).
67. Corso, M., Doccula, F. G., de Melo, J. R. F., Costa, A. & Verbruggen, N. Endoplasmic reticulum-localized CCX2 is required for osmotolerance by regulating ER and cytosolic Ca²⁺ dynamics in *Arabidopsis*. *Proc. Natl. Acad. Sci.* **115**, 3966–3971 (2018).
68. Ouziad, F., Wilde, P., Schmelzer, E., Hildebrandt, U. & Bothe, H. Analysis of expression of aquaporins and Na⁺/H⁺ transporters in tomato colonized by arbuscular mycorrhizal fungi and affected by salt stress. *Environ. Exp. Bot.* **57**, 177–186 (2006).
69. Aroca, R., Porcel, R. & Ruiz-Lozano, J. M. How does arbuscular mycorrhizal symbiosis regulate root hydraulic properties and plasma membrane aquaporins in *Phaseolus vulgaris* under drought, cold or salinity stresses?. *New Phytol.* **173**, 808–816 (2007).
70. Jahromi, F., Aroca, R., Porcel, R. & Ruiz-Lozano, J. M. Influence of salinity on the in vitro development of *Glomus intraradices* and on the in vivo physiological and molecular responses of mycorrhizal lettuce plants. *Microb. Ecol.* **55**, 45 (2008).
71. Chen, J., Zhang, H., Zhang, X. & Tang, M. Arbuscular mycorrhizal symbiosis alleviates salt stress in black locust through improved photosynthesis, water status, and K⁺/Na⁺ homeostasis. *Front. Plant Sci.* **8**, 1739 (2017).
72. Khan, M. S. The role of DREB transcription factors in abiotic stress tolerance of plants. *Biotechnol. Biotechnol. Equip.* **25**, 2433–2442 (2011).
73. Lindemose, S., O’Shea, C., Jensen, M. K. & Skriver, K. Structure, function and networks of transcription factors involved in abiotic stress responses. *Int. J. Mol. Sci.* **14**, 5842–5878 (2013).
74. Golldack, D., Li, C., Mohan, H. & Probst, N. Tolerance to drought and salt stress in plants: unraveling the signaling networks. *Front. Plant Sci.* **5**, 151 (2014).
75. Zhao, H., Jiang, J., Li, K. & Liu, G. *Populus simonii* × *Populus nigra* WRKY70 is involved in salt stress and leaf blight disease responses. *Tree Physiol.* **37**, 827–844 (2017).
76. Hu, H. *et al.* Overexpressing a NAM, ATAF, and CUC (NAC) transcription factor enhances drought resistance and salt tolerance in rice. *Proc. Natl. Acad. Sci.* **103**, 12987–12992 (2006).
77. Huang, J. *et al.* GhDREB1 enhances abiotic stress tolerance, delays GA-mediated development and represses cytokinin signalling in transgenic *Arabidopsis*. *Plant Cell Environ.* **32**, 1132–1145 (2009).
78. Shi, W. *et al.* The *Gossypium hirsutum* WRKY gene GhWRKY39-1 promotes pathogen infection defense responses and mediates salt stress tolerance in transgenic *Nicotiana benthamiana*. *Plant Cell Rep.* **33**, 483–498 (2014).
79. Qin, Y., Tian, Y. & Liu, X. A wheat salinity-induced WRKY transcription factor TaWRKY93 confers multiple abiotic stress tolerance in *Arabidopsis thaliana*. *Biochem. Biophys. Res. Commun.* **464**, 428–433 (2015).
80. Xu, Z., Wang, C., Xue, F., Zhang, H. & Ji, W. Wheat NAC transcription factor TaNAC29 is involved in response to salt stress. *Plant Physiol. Biochem.* **96**, 356–363 (2015).
81. Bi, C. *et al.* The bZIP transcription factor TabZIP15 improves salt stress tolerance in wheat. *Plant Biotechnol. J.* **19**, 209 (2021).
82. Gangappa, S. N. & Botto, J. F. The BBX family of plant transcription factors. *Trends Plant Sci.* **19**, 460–470 (2014).
83. Wen, S. *et al.* Genomic identification and expression analysis of the BBX transcription factor gene family in *Petunia hybrida*. *Mol. Biol. Rep.* **47**, 6027–6041 (2020).
84. Zhang, L. *et al.* Overexpression of a wheat MYB transcription factor gene, TaMYB56-B, enhances tolerances to freezing and salt stresses in transgenic *Arabidopsis*. *Gene* **505**, 100–107 (2012).
85. Huang, Y. *et al.* A R2R3-MYB transcription factor gene, FtMYB13, from Tartary buckwheat improves salt/drought tolerance in *Arabidopsis*. *Plant Physiol. Biochem.* **132**, 238–248 (2018).
86. Rehman, R. U. & Di Sansebastiano, G.-P. Plant Rab GTPases in membrane trafficking and signalling. In *Plant Signaling: Understanding the Molecular Crosstalk* 51–73 (2014).
87. Khassanova, G. *et al.* Intracellular vesicle trafficking genes, RabC-GTP, are highly expressed under salinity and rapid dehydration but down-regulated by drought in leaves of chickpea (*Cicer arietinum* L.). *Front. Genet.* **10**, 40 (2019).
88. Kim, H.-S. *et al.* Molecular and functional characterization of CaLEA6, the gene for a hydrophobic LEA protein from *Capsicum annuum*. *Gene* **344**, 115–123 (2005).
89. Brini, F. *et al.* Overexpression of wheat dehydrin DHN-5 enhances tolerance to salt and osmotic stress in *Arabidopsis thaliana*. *Plant Cell Rep.* **26**, 2017–2026 (2007).
90. Muvunyi, B. P. *et al.* Mining late embryogenesis abundant (LEA) family genes in *Cleistogenes songorica*, a xerophyte perennial desert plant. *Int. J. Mol. Sci.* **19**, 3430 (2018).
91. Chakrabortee, S. *et al.* Intrinsically disordered proteins as molecular shields. *Mol. Biosyst.* **8**, 210–219 (2012).
92. Qin, T., Zhao, H., Cui, P., Albeshar, N. & Xiong, L. A nucleus-localized long non-coding RNA enhances drought and salt stress tolerance. *Plant Physiol.* **175**, 1321–1336 (2017).
93. Deng, F., Zhang, X., Wang, W., Yuan, R. & Shen, F. Identification of *Gossypium hirsutum* long non-coding RNAs (lncRNAs) under salt stress. *BMC Plant Biol.* **18**, 1–14 (2018).
94. Zhang, X. *et al.* The long non-coding RNA lncRNA973 is involved in cotton response to salt stress. *BMC Plant Biol.* **19**, 1–16 (2019).
95. Zhang, W. *et al.* Identification of maize long non-coding RNAs responsive to drought stress. *PLoS ONE* **9**, e98958 (2014).

96. Sairam, R. K., Deshmukh, P. S. & Shukla, D. S. Tolerance to drought and temperature stress in relation to increased antioxidant enzyme activity in wheat. *J. Agron. Crop. Sci.* **178**, 171–177 (1997).
97. Phillips, J. M. & Hayman, D. S. Improved procedures for clearing and staining parasitic and vesicular-arbuscular mycorrhizal fungi for rapid assessment of infection. *Trans. Br. Mycol. Soc.* **55**, 158–161 (1970).
98. Giovannetti, M. & Mosse, B. An evaluation of techniques for measuring vesicular arbuscular mycorrhizal infection in roots. *New Phytol.* **84**, 489–500 (1980).
99. Ho, J., Tunkaya, T., Aryal, S., Choi, H. & Claridge-Chang, A. Moving beyond P values: Data analysis with estimation graphics. *Nat. Methods* (2019).
100. Team, R. C. R: A language and environment for statistical computing. In *R Foundation for Statistical Computing* (2021).
101. Puccio, G. *et al.* WRKY gene family drives dormancy release in onion bulbs. *Cells* **11**, 1100 (2022).
102. Andrews, S. FastQC: A quality control tool for high throughput sequence data. (2010).
103. Maccaferri, M. *et al.* Durum wheat genome highlights past domestication signatures and future improvement targets. *Nat. Genet.* **51**, 885–895 (2019).
104. Dobin, A. *et al.* STAR: Ultrafast universal RNA-seq aligner. *Bioinformatics* **29**, 15–21 (2013).
105. Liao, Y., Smyth, G. K. & Shi, W. featureCounts: An efficient general purpose program for assigning sequence reads to genomic features. *Bioinformatics* **30**, 923–930 (2014).
106. Love, M. I., Huber, W. & Anders, S. Moderated estimation of fold change and dispersion for RNA-seq data with DESeq2. *Genome Biol.* **15**, 550 (2014).
107. Thomas, P. D. *et al.* PANTHER: A library of protein families and subfamilies indexed by function. *Genome Res.* **13**, 2129–2141 (2003).
108. Kolde, R. & Kolde, M. R. Package 'pheatmap'. *R Package* **1**, <https://cran.r-project.org/web/packages/pheatmap/index.html> (2018).
109. Lohse, M. *et al.* Mercator: A Fast and Simple Web Server for Genome Scale Functional Annotation of Plant Sequence Data. (Wiley Online Library, 2014).
110. Thimm, O. *et al.* MAPMAN: A user-driven tool to display genomics data sets onto diagrams of metabolic pathways and other biological processes. *Plant J.* **37**, 914–939 (2004).
111. Williams, K. P. & Lau, B. Y. RNAcentral: A comprehensive database of non-coding RNA sequences. *Nucleic Acids Res.* **45**, (2016).
112. Supek, F., Bošnjak, M., Škunca, N. & Šmuc, T. REVIGO summarizes and visualizes long lists of gene ontology terms. *PLoS One* **6**, e21800 (2011).
113. Wickham, H. & Wickham, M. H. The ggplot package. *Google Scholar*. <http://ftp.uni-bayreuth.de/math/statlib/R/CRAN/doc/packages/ggplot.pdf> (2007).
114. Tzfadia, O. *et al.* CoExpNetViz: Comparative co-expression networks construction and visualization tool. *Front. Plant Sci.* **6**, 1194 (2016).
115. Shannon, P. *et al.* Cytoscape: A software environment for integrated models of biomolecular interaction networks. *Genome Res.* **13**, 2498–2504 (2003).
116. Kiarash, J. G. *et al.* Selection and validation of reference genes for normalization of qRT-PCR gene expression in wheat (*Triticum durum* L.) under drought and salt stresses. *J. Genet.* **97**, 1433–1444 (2018).
117. Livak, K. J. & Schmittgen, T. D. Analysis of relative gene expression data using real-time quantitative PCR and the 2⁻ΔΔCT method. *Methods* **25**, 402–408 (2001).

Author contributions

G.P., G.A., D.G., F.M. and A.S.F. conceived the study, participated in the design of the study and discussed the results critically. R.I. and D.G. performed the pot experiment and data analysis, G.P. and F.M. performed the RNA-Seq and data analysis. G.P. drafted the manuscript. G.P., R.I., F.M., G.A., D.G., F.S. and A.S.F. revised it critically. All the authors read and approved the final manuscript.

Competing interests

The authors declare no competing interests.

Additional information

Supplementary Information The online version contains supplementary material available at <https://doi.org/10.1038/s41598-022-26903-7>.

Correspondence and requests for materials should be addressed to G.P., R.I. or F.M.

Reprints and permissions information is available at www.nature.com/reprints.

Publisher's note Springer Nature remains neutral with regard to jurisdictional claims in published maps and institutional affiliations.



Open Access This article is licensed under a Creative Commons Attribution 4.0 International License, which permits use, sharing, adaptation, distribution and reproduction in any medium or format, as long as you give appropriate credit to the original author(s) and the source, provide a link to the Creative Commons licence, and indicate if changes were made. The images or other third party material in this article are included in the article's Creative Commons licence, unless indicated otherwise in a credit line to the material. If material is not included in the article's Creative Commons licence and your intended use is not permitted by statutory regulation or exceeds the permitted use, you will need to obtain permission directly from the copyright holder. To view a copy of this licence, visit <http://creativecommons.org/licenses/by/4.0/>.

© The Author(s) 2023